ELSEVIER

Journal of Organometallic Chemistry 536–537 (1997) 123–138

Journal of Organometallic Chemistry

Behaviour of triphenylphosphine-substituted ruthenium carbonyl carboxylates with hydrogen [1]

Piero Frediani [a,*], Cristina Faggi [a], Sandro Papaleo [a], Antonella Salvini [a], Mario Bianchi [a], Franco Piacenti [a], Sandra Ianelli [b], Mario Nardelli [b]

[a] *Dipartimento di Chimica Organica dell'Università di Firenze, Via Gino Capponi 9, I-50121 Firenze, Italy*

[b] *Dipartimento di Chimica Generale ed Inorganica, Chimica Analitica e Chimica Fisica, dell'Università di Parma, Centro di Studio per la Strutturistica Diffrattometrica del CNR, Viale delle Scienze 78, I-43100 Parma, Italy*

Received 20 May 1996; accepted 17 July 1996

Abstract

The reaction between $Ru(CO)_2(MeCO_2)_2(PPh_3)_2$, or $Ru_2(CO)_4(MeCO_2)_2(PPh_3)_2$, and hydrogen (100 atm) at temperatures between 80 and 160 °C has been investigated. The products formed are ruthenium clusters containing PPh_3, PPh_2 and PPh ligands. The same products were obtained from $Ru_4(\mu\text{-}H)_4(CO)_8(PPh_3)_4$ and hydrogen. Several new complexes were isolated and the crystal structures of $Ru_3(\mu\text{-}H)_2(CO)_8(\mu^3\text{-}PPh)(PPh_3)$, $Ru_4(CO)_8(\mu^4\text{-}PPh)_2(\mu\text{-}PPh_2)_2$ and $Ru_4(\mu\text{-}H)_4(CO)_7(\mu^4\text{-}PPh)(\mu\text{-}PPh_2)_2(PPh_3)$ are reported. © 1997 Elsevier Science S.A.

Keywords: Ruthenium; Carbonyl; Clusters; Hydrogen; Crystal structure

1. Introduction

The catalytic activity of ruthenium carbonyls [1] and their behaviour under reaction conditions have been investigated in our laboratory for several years [2–6]. Phosphine-substituted ruthenium carbonyls when used as catalysts in the hydrogenation under pressure of organic substrates are heavily transformed during the reaction. Carbonyl or phosphinic ligands may be displaced, carboxylato groups removed as free acids or hydrogenated to alcohols while hydridic complexes are formed. Phosphinic ligands may also react with hydrogen; rather drastic conditions, however, are necessary to modify these ligands. Tributylphosphine-substituted rutheniumcarbonyl acetates $Ru(CO)_2(MeCO_2)_2(PBu_3)_2$ and $Ru_2(CO)_4(MeCO_2)_2(PBu_3)_2$ react with hydrogen to give, through hydrogenolysis of the P–C bonds, dialkyl- or monoalkylphosphido and, in some cases, phosphido complexes in which a bare phosphorus atom is coordinated to six ruthenium atoms [3–5]. The formation of cluster complexes of higher nuclearity is, in general, associated with a relevant decrease of the catalytic activity of the system used.

Since the stability, reactivity and catalytic activity of metal complexes depends largely on the type of ligand, we have started an investigation on the behaviour of the triphenylphosphine analogue of $Ru(CO)_2(MeCO_2)_2(PBu_3)_2$ and $Ru_2(CO)_4(MeCO_2)_2(PBu_3)_2$ with hydrogen in the range of temperature 80–160 °C with the aim of comparing the behaviour of systems containing alternatively trialkyl or triarylphosphines.

2. Results

2.1. Behaviour of $Ru(CO)_2(MeCO_2)_2(PPh_3)_2$ (1) in the presence of H_2

The mononuclear ruthenium complex (**1**) reacts with hydrogen, like its tributylphosphine analogue. A reaction takes place at 100 °C giving the known dihydroruthenium complex $Ru(H)_2(CO)_2(PPh_3)_2$ (**2**). This reaction is reversible, and the position of the equilibrium depends on the hydrogen pressure and on the concentration of acetic acid in solution. When the hydrogen pressure is released the acetic acid present in solution reacts with (**2**) restoring (**1**).

Three procedures are reported in the literature for preparing complex (**2**): (a) by reacting

* Corresponding author.

[1] Dedicated to the memory of Professor Yuri Struchkov.

PII S0022-328X(96)06668-5

$Ru(CO)_2(N_2Ar)(PPh_3)_2$ (Ar = *p*-RC_6H_4, 2,6-$R'C_6H_3$, *p*-F–C_6H_4) with $NaBH_4$ [7]; (b) by substitution of a phosphine ligand in $Ru(CO)_2(PPh_3)_3$ with hydrogen [8]; (c) by displacement of a carbonyl group in $Ru(CO)_3(PPh_3)_2$ with hydrogen [9]. The last reaction, however, is reversible, and a high conversion into the dihydride is difficult to achieve.

When (**1**) is reacted with hydrogen (100 atm) at 100 °C, in the presence of sodium carbonate to neutralize the acetic acid set free, (**2**) is formed in quantitative yield (Eq. (1)). As already found in the case of the formation of the analogous tributylphosphine derivative, no intermediate monohydride complex, such as $RuH(CO)_2(MeCO_2)(PPh_3)_2$ (**3**), has been detected in this reaction.

$$\underset{\mathbf{1}}{Ru(CO)_2(MeCO_2)_2(PPh_3)_2} + 2H_2 \rightleftharpoons \underset{\mathbf{2}}{Ru(H)_2(CO)_2(PPh_3)_2} + 2MeCO_2H \quad (1)$$

A pure solution of (**2**), appropriate for a spectroscopic investigation, was prepared as described above. Its IR spectrum (absorptions at 2018(s) and 1979(s) cm^{-1}), ^1H NMR spectrum (−6.35 ppm, $^J_{HP}$ 23.4 Hz) and ^{31}P NMR spectrum (a singlet at 57.6 ppm) are all in agreement with those reported in the literature [7–9]. We have completed the spectroscopic characterization of (**2**) in order to have further support to its structure. In the ^{13}C NMR spectrum there is only one triplet at 201.7 ppm ($^J_{CP}$ 8.1 Hz) in agreement with the presence of two equivalent carbonyl groups coupling with two equivalent phosphinic ligands. These data support the structure attributed to this compound by L'Eplattenier and Calderazzo [9] on the basis of the IR data.

The hypothetical intermediate $RuH(CO)_2(MeCO_2)(PPh_3)_2$ (**3**) of the reaction between (**1**) and hydrogen has been synthesized by reacting (**2**) with acetic acid (Eq. (2)).

$$\underset{\mathbf{2}}{Ru(H)_2(CO)_2(PPh_3)_2} + MeCO_2H \rightleftharpoons \underset{\mathbf{3}}{RuH(CO)_2(MeCO_2)(PPh_3)_2} + H_2 \quad (2)$$

At room temperature the complete conversion of (**2**) into (**3**) is achieved in 6 h. The reaction is first order with respect to the concentration of (**2**) with a specific rate of 1.8×10^{-4} mol s^{-1} at 20 °C. This new complex has been characterized in solution by IR and multinuclear NMR spectroscopy. The singlet at 46.5 ppm in the ^{31}P NMR spectrum is in agreement with two equivalent phosphinic ligands. In the ^1H NMR spectrum there is only one triplet at −3.68 ppm ($^J_{HP}$ 19.2 Hz), in agreement with a hydridic hydrogen coupling with two equivalent phosphinic ligands. The value of the coupling constant agrees with a cis position of the hydridic hydrogen with respect to the phosphines. Two triplets at 206.3 ppm ($^J_{CP}$ 14.3 Hz) and 207.5 ppm ($^J_{CP}$ 17.2 Hz) are present in the ^{13}C NMR spectrum which may be attributed to two non-equivalent carbonyl groups coupling with two equivalent phosphinic ligands. A resonance at 184.0 ppm may be attributed to the carboxylato group of the acetato ligand. The presence of two absorptions with the same intensity at 2045(s) and 1970(s) cm^{-1} in the carbonyl stretching region of the IR spectrum are in keeping with the formation of (**3**) having an octahedral structure with two phosphines in trans position and two carbonyl groups in cis position.

The monohydride (**3**) reacts with an excess of acetic acid at room temperature giving (**1**) and hydrogen. This reaction may be monitored by multinuclear NMR and the formation of hydrogen in solution may by confirmed by the resonance at 4.5 ppm in the ^1H NMR spectrum.

The transformation of (**3**) into (**1**) (Eq. (3)) is first order with respect to the concentration of (**3**), with a specific rate of 3×10^{-5} mol s^{-1} at 50 °C.

$$\underset{\mathbf{3}}{RuH(CO)_2(MeCO_2)(PPh_3)_2} + MeCO_2H \rightleftharpoons \underset{\mathbf{1}}{Ru(CO)_2(MeCO_2)2(PPh_3)_2} + H_2 \quad (3)$$

The dihydride (**2**) reacts with two equivalents of acetic acid at room temperature. The complete transformation of (**2**) into (**1**) and hydrogen is reached in 2 h at 50 °C. At this temperature an almost complete transformation of (**2**) into (**3**) is noticed after a few minutes; (**1**) starts to be present almost from the beginning (Scheme 1).

2.2. Behaviour of $Ru_2(CO)_4(MeCO_2)_2(PPh_3)_2$ (4) with H_2

The behaviour of (**4**) in cyclohexane solution, under H_2 pressure (100 atm), has been examined in the temperature range 80–140 °C.

The reaction conditions and the main products formed are reported in Table 1. A semiquantitative evaluation

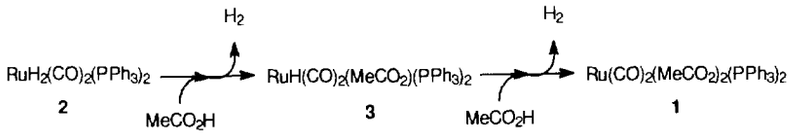

Scheme 1.

Table 1
Behaviour of $Ru_2(CO)_4(MeCO_2)_2(PPh_3)_2$ (**4**) with hydrogen [a]

Test no.	T (°C)	t (h)	Identified products (yield)
1 [b]	140	24	(**5**)(5±2), (**6**)(10±2), (**7**)(5±2), (**8**)(15±2)
2 [b]	140	72	(**5**)(5±2), (**6**)(10±2), (**7**)(10±2), (**8**)(15±2)
3 [c]	140	72	(**6**)(10±2), (**7**)(10±2), (**8**)(10±2)
4 [c]	120	72	(**6**)(5±2), (**8**)(15±2)
5 [c]	100	72	(**6**)(5±2), (**8**)(15±2)
6 [c]	80	72	(**8**)(2±2), (**10**)(15±2), (**4**)(10±2)

[a] The yields have been evaluated by the spots of the complexes in the tlc analyses. [b] (**4**) 250 mg, cyclohexane (30 ml), p_{H_2} 100 atm. [c] (**4**) 50 mg, C_6D_6 (3 ml), Na_2CO_3 (300 mg), p_{H_2} 100 atm.

of the amount of the products formed is reported, and refers to the relative amounts appearing in the tlc analyses.

Several products are formed, and the chemioselectivity never exceeds 15% of the total. The main products are $Ru_3(\mu\text{-}H)_2(CO)_8(\mu^3\text{-}PPh)(PPh_3)$ (**5**), $Ru_3(\mu\text{-}H)(H)(CO)_7(\mu\text{-}PPh_2)_2(PPh_3)$ (**6**), $Ru_4(CO)_8(\mu^4\text{-}PPh)_2(\mu\text{-}PPh_2)_2$ (**7**), $Ru_4(\mu\text{-}H)_4(CO)_7(\mu^4\text{-}PPh)(\mu\text{-}PPh_2)_2(PPh_3)$ (**8**). They have been separated by preparative tlc and purified by crystallization from CH_2Cl_2–pentane solutions by cooling at −20 °C.

The structures of (**5**), (**7**), and (**8**) have been determined by single crystal X-ray diffractometry. Compound (**6**) has been identified and characterized through its spectroscopic data. The mass spectrum of the complex, in the range between 800–1300 m/e, has a molecular peak at 1134 m/e and a base peak at 1106 m/e. Peaks corresponding to the loss of seven carbonyl groups are observed. The IR and multinuclear NMR data support the formulation proposed and will be discussed later. The number of hydrogen atoms present in the complexes (**5**)–(**8**) was determined by integration of the hydridic resonance, in the ^1H NMR spectrum, of solutions of known amounts of the complex to be examined and of $Ru_4(\mu\text{-}H)_4(CO)_8(PPh_3)_4$ (**9**).

In consideration of the fact that complexes containing carboxylato groups have never been detected among these reaction products, the displacement of acetic acid seems to be the first step of this reaction. In order to ease the reaction between (**4**) and hydrogen, we have carried out a series of experiments in the presence of sodium carbonate. C_6D_6 was used as solvent in order to be able to analyse directly, without any manipulations, the crude of the reaction by NMR spectroscopy.

The products formed in these conditions are the same as those obtained in the absence of sodium carbonate. The reaction occurs at a lower temperature (40 °C) than that necessary in the absence of the base. These experiments confirm that, as in the case of the mononuclear compound (**1**), the first step of this reaction is the coordination of hydrogen followed by the loss of acetic acid.

The main product formed when (**4**) is heated at 80 °C in the presence of hydrogen and sodium carbonate is the hydride $Ru_4(\mu\text{-}H)_4(CO)_9(PPh_3)_3$ (**10**). The formation of (**5**), (**6**), (**7**) and (**8**) takes place when (**4**) is heated, in the presence of hydrogen, at higher temperatures.

Since (**10**) is the main product of the reaction between (**4**) and hydrogen at low temperature (80 °C) and (**10**) may be derived from (**9**) in the presence of carbon monoxide [10] (Eq. (4)), it seems reasonable to suggest that (**10**) or (**9**) are the products formed when reacting the carboxylato complex (**4**) and hydrogen.

$$\underset{\mathbf{9}}{Ru_4(\mu\text{-}H)_4(CO)_8(PPh_3)_4} + CO \rightleftharpoons \underset{\mathbf{10}}{Ru_4(\mu\text{-}H)_4(CO)_9(PPh_3)_3} + PPh_3 \quad (4)$$

Furthermore, the structure of (**8**) suggests that it is very likely formed from (**9**) by hydrogenolysis of the aryl group of the phosphine ligands. Also (**7**) is a cluster containing four ruthenium atoms and it may derive from (**9**).

These hypotheses were checked by studying the reaction between (**9**) and hydrogen.

2.3. Behaviour of $Ru_4(\mu\text{-}H)_4(CO)_8(PPh_3)_4$ (9) with H_2

These experiments were carried out using the same procedure reported for (**4**). The conditions adopted and the results obtained are reported in Table 2.

It is possible to conclude that the products formed from (**4**) or (**9**) are the same, even if in different amounts. These results confirm the hypothesis that the first transformation of (**4**) produces (**9**). Several rearrangements then take place and other products are formed.

The reaction temperature plays the main role in this reaction; the hydrogen pressure (above 100 atm), however, does not seem to have a relevant effect on the types of product formed.

Table 2
Behaviour of $Ru_4(\mu\text{-}H)_4(CO)_8(PPh_3)_4$ (**9**) with hydrogen [a]

Test no.	T (°C)	t (h)	p_{H_2} (atm)	Identified products
7	140	72	100	(**5**)(5±2), (**6**)(10±2), (**7**)(10±2) (**8**)(15±2)
8	140	72	150	(**6**)(10±2), (**7**)(5±2), (**8**)(10±2)
9	160	96	100	(**6**)(5±2), (**7**)(10±2)
10	160	96	210	(**7**)(10±2)
11 [b]	160	72	100	(**6**)(5±2), (**7**)(10±2)

[a] (**9**) 100 mg, solvent (C_6H_{12}) 10 ml; the yields have been evaluated by the spots of the complexes in the tlc analyses. [b] Solvent $C_{10}H_{18}$.

Test 11 has been carried out using decaline as solvent in order to be able to detect the possible formation of cyclohexane or benzene due to the hydrogenation and/or hydrogenolysis of the PPh_3 ligand. The gas chromatographic analysis confirms the formation of benzene and the absence of cyclohexane among the products of this reaction.

2.4. Crystal structure determination

2.4.1. Molecular structure of $Ru_3(\mu\text{-}H)_2(CO)_8(\mu^3\text{-}PPh)(PPh_3)$ (5)

Fig. 1 shows the ORTEP [11] drawing of the molecule of compound (**5**), which consists of a central triangular closed-shell 48-electron metal cluster, capped by a μ^3-

Table 3
Relevant bond distances (Å), bond angles (deg) and torsion angles (deg) of compound (**5**): $Ru_3(\mu\text{-}H)_2(CO)_8(\mu^3\text{-}PPh)(PPh_3)$

Ru1–Ru2	2.835(2)	Ru1–Ru3	2.958(2)	Ru3–P1	2.388(3)
		Ru2–Ru3	2.950(2)		
Ru3–P2	2.303(3)	av.	2.954(2)	Ru2–C5C	1.924(16)
Ru2–P2	2.291(4)			Ru1–C1C	1.918(16)
Ru1–P2	2.288(4)	Ru2–C6C	1.953(14)	av.	1.921(11)
av.	2.295(5)	Ru1–C3C	1.935(14)		
		av.	1.943(10)	Ru1–C2C	1.908(13)
Ru3–C8C	1.860(16)			Ru2–C4C	1.898(13)
Ru3–C7C	1.846(15)	P1–C13	1.841(14)	av.	1.903(9)
av.	1.853(11)	P1–C19	1.833(13)		
		P1–C7	1.823(14)	C–O av.	1.133(6)
P2–C1	1.800(13)	av.	1.832(8)	C–C av.	1.387(5)
Ru1–Ru2–Ru3	61.45(5)	Ru1–Ru3–Ru2	57.36(4)	Ru1–Ru3–P1	114.30(9)
Ru2–Ru1–Ru3	61.19(4)			Ru2–Ru3–P1	111.70(9)
av.	61.3(1)	Ru3–Ru2–P2	50.23(9)	av.	113.0(13)
		Ru3–Ru1–P2	50.13(9)		
Ru2–Ru1–P2	51.80(9)	av.	50.18(6)	Ru1–Ru3–C7C	147.9(4)
Ru1–Ru2–P2	51.70(9)			Ru3–Ru1–C2C	145.3(4)
av.	51.75(6)	Ru2–Ru3–P2	49.88(9)	Ru2–Ru3–C8C	144.9(5)
		Ru1–Ru3–P2	49.68(9)	Ru3–Ru2–C4C	144.8(4)
Ru2–Ru1–C1C	160.4(5)	av.	49.78(10)	av.	145.8(8)
Ru1–Ru2–C5C	158.1(5)				
av.	159.2(12)	Ru3–Ru2–C6C	110.9(4)	Ru3–Ru1–C1C	101.3(4)
		Ru3–Ru1–C3C	110.0(4)	Ru3–Ru2–C5C	101.1(5)
		av.	110.4(4)	av.	101.2(3)
Ru2–Ru3–C7C	100.9(4)	Ru2–Ru1–C3C	93.7(4)	C5C–Ru2–C6C	104.0(6)
Ru2–Ru1–C2C	95.8(4)	Ru1–Ru2–C4C	93.4(4)	C1C–Ru1–C3C	101.1(6)
Ru2–Ru1–C6C	95.1(4)	Ru1–Ru3–C8C	93.8(4)	av.	102.6(14)
		av.	93.6(4)		
Ru1–P2–Ru3	80.2(1)	Ru1–P2–C1	135.0(4)	Ru3–P1–C13	116.7(4)
Ru2–P2–Ru3	79.9(1)	Ru3–P2–C1	132.1(4)	Ru3–P1–C19	115.4(4)
Ru1–P2–Ru2	76.5(1)	Ru2–P2–C1	131.3(5)	Ru3–P1–C7	113.0(4)
av.	78.9(12)	av.	132.9(11)	av.	114.9(11)
P2–Ru1–C1C	111.0(5)	P2–Ru2–C4C	95.2(4)	P2–Ru2–C6C	145.9(4)
P2–Ru2–C5C	107.4(5)	P2–Ru1–C2C	95.4(4)	P2–Ru1–C3C	144.5(4)
av.	109.3(18)	av.	95.3(3)	av.	145.1(7)
C2C–Ru1–C3C	96.4(6)	P2–Ru3–C7C	98.5(4)	P1–C7–C12	122.9(10)
C1C–Ru1–C2C	95.2(6)	P2–Ru3–C8C	97.1(5)	P1–C19–C20	122.7(10)
C4C–Ru2–C6C	94.6(6)	P1–Ru3–C8C	97.7(5)	P1–C13–C14	122.5(11)
C4C–Ru2–C5C	95.6(6)	P1–Ru3–C7C	95.1(4)	P2–C1–C2	121.6(10)
C7C–Ru3–C8C	94.9(6)	av.	97.1(8)	av.	122.4(5)
av.	95.4(3)				
P2–C1–C6	120.0(11)	P1–Ru3–P2	159.0(1)	C–C(*i*)–C av.	118.3(6)
P1–C13–C18	120.0(11)	Ru–C–O av.	177.1(8)	C–C(*m*)–C av.	119.5(6)
P1–C7–C8	118.5(10)	C–P–C av.	103.4(8)	C–C(*o*)–C av.	120.4(7)
P1–C19–C24	118.4(10)			C–C(*p*)–C av.	121.7(9)
av.	119.2(5)				
Ru1–P2–C1–C2	167.2(9)			Ru2–P2–C1–C6	−127.0(11)
Ru3–P2–C1–C2	−67.4(14)			Ru3–P1–C7–C8	67.6(11)
Ru3–P1–C13–C14	−139.7(11)			Ru3–P1–C19–C20	−140.5(10)
		C6–C1...P1–C7	−61.8(13)		

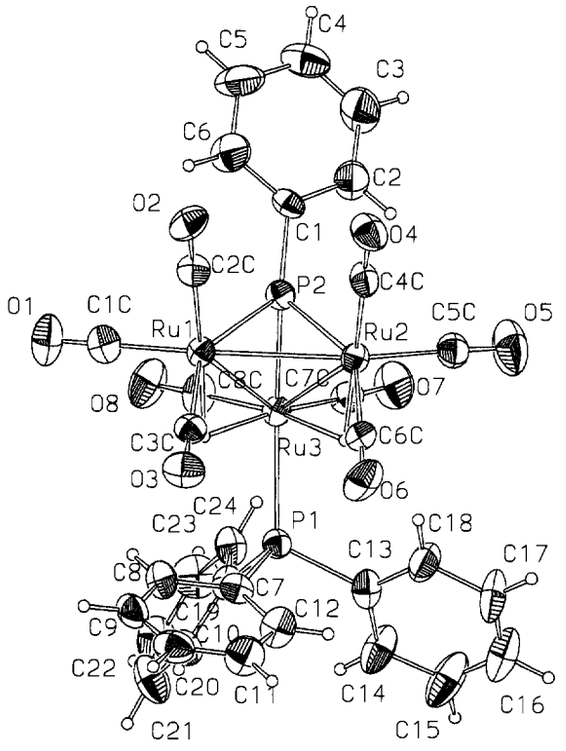

Fig. 1. ORTEP projection of the structure of $Ru_3(\mu\text{-}H)_2(CO)_8(\mu^3\text{-}PPh)(PPh_3)$ (**5**). Ellipsoids at 30% probability level.

monophenylphosphido ligand with two sides bridged by two hydrides. A terminal triphenylphosphine coordinates to the Ru atom involved in both hydrido bridges. Coordination about the Ru atoms is completed by terminal carbonyls: two bound to the ruthenium atom carrying the terminal phosphine, and three bound to each of the other metal atoms. So, there are two kinds of Ru atom: two (Ru1 and Ru2) heptacoordinated, and one (Ru3) octacoordinated.

The relevant structural parameters of the molecule are quoted in Table 3, where averaged values are also given (for all the three structures described in this paper, averages are considered when averaging can have some meaning). All the values are near to those expected [12,13]. It is worth noting that, as found in other μ-hydrido clusters, there are two kinds of Ru–Ru distance, one shorter (2.835(2) Å) the other longer (av. 2.954(2) Å), respectively corresponding to the sides unsubtended and subtended by the hydrido bridges. Concerning the endocyclic angles in the cluster, it must be noted that the angle at Ru3 (carrying the terminal phosphine) is significantly narrower (57.36(4)°) than those at the other ruthenium atoms (av. 61.3(1)°).

The orientations of the four phenyl rings of compound (**5**) are defined by the torsion angles quoted in Table 3. The non-bonded energy profiles, calculated for isolated molecules by using the ROTENER program [14] for rotations of the phenyl rings about the P–C bonds, show that the phenyl of the μ^3-P2 phosphido ligand can rotate without significant intramolecular energy barriers (energies less than 3.5 kJ mol^{-1}, contacts less than 2.8 Å) with two minima: one is -4.7 kJ mol^{-1} at $-100°$, the other is -6.4 kJ mol^{-1} at 75° (positive rotations are

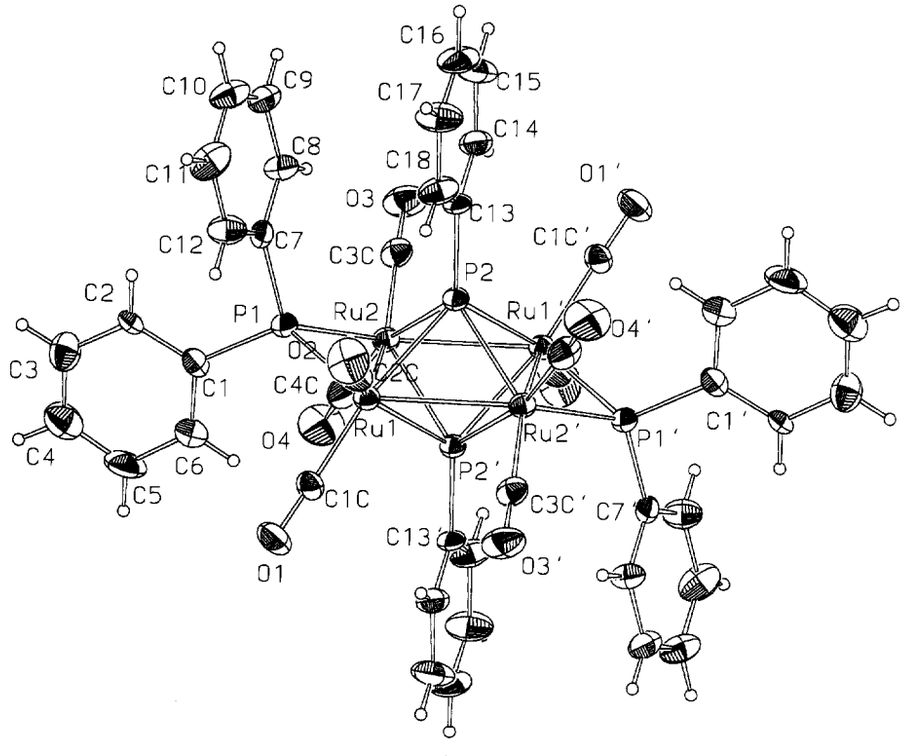

Fig. 2. ORTEP projection of the structure of $Ru_4(CO)_8(\mu^4\text{-}PPh)_2(\mu\text{-}PPh_2)_2$ (**7**). Ellipsoids at 30% probability level.

counterclockwise) with respect to the experimentally observed conformation (assumed for the zero of energy); this is therefore determined by packing interactions. The rings of triphenylphosphine are much less free, their rotation being hindered by intramolecular repulsive interactions that, in the case of phenyl C7, involve its *ortho*- and *meta*-hydrogen atoms and the C3C–O3 carbonyl, the H13-hydride and an *ortho*-hydrogen of the adjacent phenyl C19, while, in the case of phenyls C13 and C19, hindering involves their *ortho*-hydrogen atoms with H12 and H14 of the C7 and C13 phenyls respectively.

Table 4
Relevant bond distances (Å), bond angles (deg) and torsion angles (deg) of compound (7): $Ru_4(CO)_8(\mu^4\text{-PPh})_2(\mu\text{-PPh}_2)_2$ (′: $1-x,-y,-z$)

Ru1–Ru2	2.767(2)	Ru1–P2	2.452(3)	Ru1–P1	2.306(3)
Ru1–Ru2′	2.866(2)	Ru2–P2	2.446(3)	Ru2–P1	2.311(3)
		Ru1–P2′	2.418(3)	av.	2.309(2)
Ru1–C2C	1.893(8)	Ru2–P2′	2.424(3)		
Ru2–C3C	1.870(11)	av.	2.434(8)	P1–C1	1.828(12)
Ru1–C1C	1.879(13)			P2–C13	1.811(10)
Ru2–C4C	1.875(10)	C–O av.	1.135(6)	P1–C7	1.809(11)
av.	1.882(6)	C–C av.	1.384(4)	av.	1.815(6)
Ru2–Ru1–Ru2′	90.00(4)	Ru2′–Ru1–P1	137.07(8)	Ru1–Ru2–P2	55.71(6)
Ru1–Ru2–Ru1′	90.00(3)	Ru1′–Ru2–P1	136.95(8)	Ru2–Ru1–P2	55.49(6)
av.	90.00(4)	av.	137.01(6)	Ru2–Ru1–P2′	55.26(6)
				Ru1–Ru2–P2′	55.04(6)
Ru1–P2–Ru1′	109.76(09)	Ru1–P1–Ru2	73.64(8)	Ru1–Ru2′–P2	54.46(7)
Ru2–P2–Ru2′	109.76(11)	Ru2–P2–Ru1′	72.19(8)	Ru2–Ru1′–P2	54.35(6)
av.	109.76(7)	Ru1–P2–Ru2′	71.98(8)	Ru2′–Ru1–P2	53.56(7)
		Ru1–P2′–Ru2	69.70(7)	Ru1′–Ru2–P2	53.45(7)
		Ru1–P2–Ru2	68.80(7)	Ru2–Ru1–P1	53.26(7)
		av.	71.0(9)	Ru1–Ru2–P1	53.10(7)
				av.	54.5(3)
Ru1–Ru2–C3C	147.0(3)	Ru2′–Ru1–C1C	119.6(3)	Ru2′–Ru1–C2C	90.8(4)
Ru2–Ru1–C2C	145.7(3)	Ru1–Ru2–C4C	118.1(4)	Ru1′–Ru2–C3C	90.3(3)
av.	146.4(7)	Ru1′–Ru2–C4C	118.3(4)	av.	90.5(2)
		Ru2–Ru1–C1C	117.4(3)		
		av.	118.3(5)		
C1C–Ru1–C2C	91.6(5)	P2–Ru1–C1C	167.3(3)	P2′–Ru1–C2C	143.7(3)
C3C–Ru2–C4C	90.4(5)	P2–Ru2–C4C	166.8(4)	P2′–Ru2–C3C	143.0(3)
av.	91.1(6)	av.	167.1(2)	av.	143.3(3)
P1–Ru1–C2C	107.5(4)	P1–Ru1–C1C	98.8(3)	P2′–Ru1–C1C	97.1(3)
P1–Ru2–C3C	108.8(3)	P2–Ru1–C2C	98.9(3)	P2′–Ru2–C4C	96.6(4)
av.	108.3(7)	av.	98.8(2)	av.	96.9(2)
P2–Ru1–C1C	167.3(3)	P2′–Ru1–C2C	143.7(3)		
P2–Ru2–C4C	166.8(4)	P2′–Ru2–C3C	143.0(3)		
av.	167.1 (3)	av.	143.3(3)		
P1–Ru2–C4C	100.2(4)	P2–Ru2–C3C	99.4(4)	Ru1–C1C–O1	179.0(10)
P2–Ru2–C3C	99.4(3)	P2′–Ru2–C4C	96.6(4)	Ru1–C2C–O2	179.2(10)
av.	99.8(4)	av.	98.0(14)	Ru2–C3C–O3	178.0(10)
				Ru2–C4C–O4	176.6(12)
				av.	178.3(5)
P1–Ru1–P2′	105.93(10)	P1–Ru1–P2	84.84(10)	P2–Ru1–P2′	70.24(8)
P1–Ru2–P2′	105.58(10)	P1–Ru2–P2	84.88(9)	P2–Ru2–P2′	70.24(9)
av.	105.7(2)	av.	84.86(7)	av.	70.24(6)
Ru1–P2–C13	125.9(4)	Ru1–P1–C1	121.6(4)	C1–P1–C7	103.4(5)
Ru2′–P2–CI3	125.3(4)	Ru2–P1–C7	121.0(3)	P–C–C av.	120.8(5)
Ru2–P2–C13	124.9(4)	Ru2–P1–C1	119.9(3)	C–C(*i*)–C av.	118.4(6)
Ru1′–P2–C13	124.4(3)	Ru1–P1–C7	116.5(4)	C–C(*o*)–C av.	120.5(6)
av.	125.1(3)	av.	119.8(11)	C–C(*m*)–C av.	119.9(7)
				C–C(*p*)–C av.	120.5(11)
Ru1–P1–C1–C2	133.3(9)	Ru2–P1–C7–C8	27.7(12)		
Ru2–P1–C1–C6	42.0(12)	Ru1–P2–C13–C14	−141.8(9)		
Ru1–P1–C7–C12	−62.6(11)	Ru2–P2–C13–C18	124.3(10)		

2.4.2. Molecular structure of $Ru_4(CO)_8(\mu^4\text{-}PPh)_2(\mu\text{-}PPh_2)_2$ (7)

As shown in Fig. 2, the molecule of compound (**7**) consists of a square closed-shell 62-electron metal cluster of ruthenium atoms capped by two μ^4-monophenylphosphido ligands lying on opposite sides with respect to the plane of the square. Two bridging μ-diphenylphosphido ligands span two opposite sides of the square. Coordination about each metal atom is completed to seven by two terminal carbonyls. The whole molecule lies on a crystallographic centre of symmetry.

Table 4 shows the relevant geometric parameters of the molecule, whose values agree well with the averages in the literature [12,13]. The two independent Ru–Ru distances deviate significantly from being equal; the shorter is that bridged by the μ-diphenylphosphido ligand. On the contrary, the two independent endocyclic angles of the metal cluster are both exactly equal to 90°.

The torsion angles of Table 4 define the orientations of the three independent phenyls present in compound (**7**). The non-bonded energy profiles show that the less hindered phenyl is that of C1, for which the largest barrier does not exceed 18 kJ mol^{-1} and no interatomic contact is less than 2.14 Å, the hindering being due to its *ortho*-hydrogen atoms and the C1C–O1 and C4C–O4 carbonyls. The other two phenyls show much larger barriers, mainly due to the interactions between their *ortho*-hydrogen atoms and the *ortho*-hydrogen atoms of adjacent phenyls (H12 and H8 with H2; H14 and H18 with H8).

2.4.3. Molecular structure of $Ru_4(\mu\text{-}H)_4(CO)_7(\mu^4\text{-}PPh)(\mu\text{-}PPh_2)_2(PPh_3)$ (8)

The molecule of compound (**8**), represented in the ORTEP projection of Fig. 3, is built by a central square closed-shell 62-electron metal cluster of ruthenium atoms capped by a μ^4-monophenylphosphido ligand and bridged on opposite sides by two μ-diphenylphosphido ligands. All sides of the square are spanned by μ-hydrides all displaced from the plane of the square in the same direction opposite to that of the μ^4-PPh ligand. Two terminal carbonyls coordinate to each metal atom, except that one of them (Ru3) which has a coordination site occupied by a terminal triphenylphosphine at the place of a carbonyl. In this way, all the Ru atoms reach the same coordination number of eight.

Concerning the geometric parameters (Table 5), it must be noted that for compound (**8**) the agreement with the averages of the literature [12,13] is better, confirming the better accuracy of the analysis indicated by the values of the *R* indices quoted in Table 6. Also, in this case, two kinds of Ru–Ru distances are observed: one shorter (av. 2.828(2) Å) corresponding to the sides spanned by the bridging PPh_2 phosphido ligands, the other longer (av. 2.964(12) Å) related to the other opposite sides. Differences of about 1° are also present in the endocyclic angles of the metal cluster: the angles at Ru1 and Ru3 are narrower (av. 89.4(3)°) while those at Ru2 and Ru4 are larger (av. 90.5(2)°) than 90°.

In the molecule of compound (**8**) eight phenyls are present; one of them, C27, is conformationally disor-

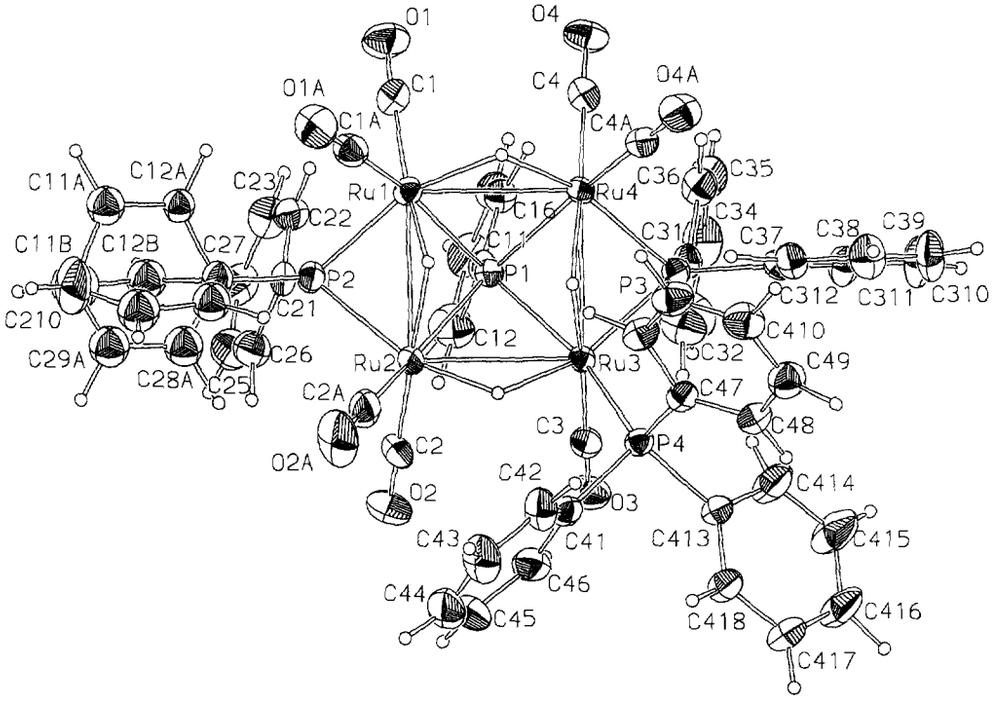

Fig. 3. ORTEP projection of the structure of $Ru_4(\mu\text{-}H)_4(CO)_7(\mu^4\text{-}PPh)(\mu\text{-}PPh_2)_2(PPh_3)$ (**8**). Ellipsoids at 30% probability level.

Table 5
Relevant bond distances (Å), bond angles (deg) and torsion angles (deg) of compound (**8**): $Ru_4(\mu\text{-}H)_4(CO)_7(\mu^4\text{-}PPh)(\mu\text{-}PPh_2)_2(PPh_3)$

Ru1–Ru2	2.830(1)	Ru4–C4A	1.864(7)	Ru2–P2	2.315(2)
Ru3–Ru4	2.825(1)	Ru3–C3	1.868(7)	Ru3–P3	2.319(2)
av.	2.828(2)	Ru4–C4	1.885(7)	Ru3–P4	2.323(2)
		Ru2–C2	1.886(8)	Ru1–P2	2.330(2)
Ru1–Ru4	2.977(1)	Ru1–C1A	1.888(7)	Ru4–P3	2.349(2)
Ru2–Ru3	2.952(1)	Ru2–C2A	1.888(8)	av.	2.327(6)
av.	2.964(12)	Ru1–C1	1.891(8)		
		av.	1.881(4)	P–C av.	1.830(4)
Ru2–P1	2.429(2)			C–O av.	1.141(4)
Ru3–P1	2.439(2)			C–C av.	1.381(4)
Ru1–P1	2.447(2)				
Ru4–P1	2.473(2)				
av.	2.447(9)				
Ru1–Ru2–Ru3	90.76(3)	Ru2–Ru3–Ru4	89.73(3)	Ru2–Ru3–P3	136.72(5)
Ru1–Ru4–Ru3	90.33(3)	Ru2–Ru1–Ru4	89.13(3)	Ru1–Ru4–P3	135.63(5)
av.	90.5(2)	av.	89.4(3)	Ru3–Ru2–P2	135.34(5)
				Ru4–Ru1–P2	134.47(5)
				av.	135.5(5)
Ru4–Ru3–P4	124.51(5)	Ru1–Ru2–P1	54.81(5)	Ru4–Ru1–C1A	124.0(2)
Ru2–Ru3–P4	111.18(5)	Ru4–Ru3–P1	55.46(4)	Ru1–Ru4–C4A	122.5(2)
		Ru3–Ru4–P1	54.34(4)	Ru3–Ru2–C2A	119.5(2)
Ru1–Ru2–C2	145.5(3)	Ru2–Ru1–P1	54.24(5)	Ru3–Ru4–C4A	117.5(2)
Ru2–Ru1–C1	114.5(2)	Ru4–Ru3–P3	53.24(5)	Ru1–Ru2–C2A	113.6(3)
Ru3–Ru4–C4	144.0(2)	Ru4–Ru1–P1	53.17(4)	Ru2–Ru1–C1A	113.5(2)
Ru4–Ru3–C3	142.0(2)	Ru3–Ru2–P1	52.84(4)	av.	118.9(17)
av.	143.8(7)	Ru1–Ru2–P2	52.71(5)		
		Ru2–Ru3–P1	52.52(4)	Ru4–Ru1–C1	95.5(2)
P1–Ru3–P3	85.43(6)	Ru1–Ru4–P1	52.35(5)	Ru2–Ru3–C3	95.2(2)
P1–Ru4–P3	84.04(6)	Ru3–Ru4–P3	52.28(5)	Ru3–Ru2–C2	94.4(2)
P1–Ru2–P2	83.09(6)	Ru2–Ru1–P2	52.24(5)	Ru1–Ru4–C4	93.7(2)
P1–Ru1–P2	82.41(6)	av.	53.4(3)	av.	94.7(4)
av.	83.7(6)				
P1–Ru3–P4	162.28(6)	C2–Ru2–C2A	93.2(3)	P3–Ru4–C4	104.1(2)
P3–Ru3–P4	108.69(7)	C1–Ru1–C1A	92.9(3)	P2–Ru2–C2	103.3(2)
		C4–Ru4–C4A	90.0(3)	P1–Ru2–C2	103.1(2)
P1–Ru4–C4A	167.2(2)	av.	92.0(10)	P2–Ru1–C1	103.9(2)
P1–Ru1–C1A	165.2(2)			P3–Ru3–C3	102.0(2)
P1–Ru2–C2A	162.2(2)	Ru2–P1–C11	125.3(2)	P1–Ru1–C1	101.8(2)
av.	164.9(14)	Ru3–P3–C37	124.6(2)	P1–Ru4–C4	101.8(2)
		Ru3–P1–C11	123.1(2)	P2–Ru2–C2A	100.3(2)
		Ru4–P1–C11	122.2(2)	P1–Ru3–C3	99.1(2)
		Ru1–P1–C11	122.1(2)	P3–Ru4–C4A	98.2(2)
Ru1–P1–Ru3	114.79(7)	Ru1–P2–C21	120.9(2)	P2–Ru1–C1A	96.0(2)
Ru2–P1–Ru4	112.49(7)	Ru2–P2–C27	120.7(2)	P4–Ru3–C3	88.6(2)
av.	113.6(12)	Ru1–P2–C27	120.4(2)	av.	100.2(13)
		Ru3–P3–C31	119.4(2)		
Ru1–P2–Ru2	75.06(6)	Ru4–P3–C37	118.5(2)	Ru–C–O av.	178.4(2)
Ru2–P1–Ru3	74.64(5)	Ru2–P2–C21	118.1(2)	C–P–C av.	102.7(3)
Ru3–P3–Ru4	74.48(5)	Ru3–P4–C413	118.3(2)	P–C–C av.	121.0(4)
Ru1–P1–Ru4	74.48(5)	Ru3–P4–C47	117.7(2)	C–C(*i*)–C av.	117.8(3)
Ru1–P1–Ru2	70.95(5)	Ru4–P3–C31	116.0(2)	C–C(*o*)–C av.	120.5(2)
Ru3–P1–Ru4	70.20(5)	Ru3–P4–C41	109.9(2)	C–C(*m*)–C av.	120.7(4)
av.	73.2(9)	av.	119.8(10)	C–C(*p*)–C av.	119.4(4)
Ru1–P1–C11–C12	−114.9(5)	Ru2–P2–C27–C28B	28.5(11)		
Ru2–P1–C11–C12	−26.5(6)	Ru3–P3–C31–C32	−39.9(6)		
Ru3–P1–C11–C12	67.7(6)	Ru4–P3–C31–C32	−126.1(6)		
Ru4–P1–C11–C12	153.9(4)	Ru3–P3–C37–C38	131.1(5)		
Ru1–P2–C21–C22	−26.4(7)	Ru4–P3–C37–C38	−138.6(5)		
Ru2–P2–C21–C22	−115.2(6)	Ru3–P4–C41–C42	−112.2(6)		
Ru1–P2–C27–C28A	−130.4(9)	Ru3–P4–C47–C48	−136.2(5)		
Ru2–P2–C27–C28A	−40.3(10)	Ru3–P4–C413–C414	40.2(6)		
Ru1–P2–C27–C28B	−61.5(10)				

Table 6
Experimental data for the X-ray analysis of $Ru_3(\mu\text{-}H)_2(CO)_8(\mu^3\text{-}PPh)(PPh_3)$ (**5**), $Ru_4(CO)_8(\mu^4\text{-}PPh)_2(\mu\text{-}PPh_2)_2$ (**7**), and $Ru_4(\mu\text{-}H)_4(CO)_8(\mu^4\text{-}PPh)(\mu\text{-}PPh_2)_2(PPh_3)$ (**8**)

Compound	(5)	(7)	(8)
Formula	$C_{32}H_{22}O_8P_2Ru_3$	$C_{44}H_{30}O_8P_4Ru_4$	$C_{55}H_{44}O_7P_4Ru_4$
M	899.65	1214.89	1345.12
Space group	$P2_1/a$	$P-1$	$P2_1/n$
a/Å	18.435(12)	11.170(6)	22.340(10)
b/Å	17.594(11)	11.716(5)	18.149(9)
c/Å	10.739(6)	10.167(3)	13.950(6)
α/deg	90.0	114.85(4)	90.0
β/deg	99.18(3)	102.65(4)	104.91(2)
γ/deg	90.0	102.11(3)	90.0
U/Å^3	3438(4)	1107.5(8)	5466(4)
Z	4	1	4
D_x/Mg m^{-3}	1.738	1.822	1.635
$F(000)$	1760	594	2664
Crystal size/mm^3	0.22 × 0.28 × 0.36	0.14 × 0.32 × 0.37	0.23 × 0.46 × 0.65
μ/mm^{-1}	1.44	1.53	1.25
Diffractometer	Siemens-AED	Nonius-CAD4	Nonius-CAD4
No. of reflections for cell parameters	23	25	25
θ range for cell parameters/deg	11.1/17.7	11.5/18.4	9.3/12.3
θ-range for intensity collection/deg	3.0/28.0	3.1/30.0	3.0/28.0
h range	−24/24	−15/15	−24/24
k range	−23/0	−16/14	23/0
l range	−14/0	0/14	−14/14
Standard reflection(s)	−5 2 4	4 −5 3	9 3 3/−2 5 7
Intensity variation	< 0.1%	< 0.1%	< 0.1%
No. of measured reflections	8985	6191	10356
No. of unique reflections	8056	6191	5880
R(int)	0.0825	—	0.0233
Refinement on	F^2	F^2	F
No. of reflections used in the refinement (N)	8052	6181	5622
No. of observed reflections ($I > 2\sigma(I)$)	3190	2887	3190
No. of refined parameters (P)	414	271	552
Max. LS shift to e.s.d. ratio	−0.006	< 0.001	−0.006
Min./max. height in final $\Delta\rho$ map/e Å^{-3}	−1.17/1.63	−1.14/2.52	−0.19/0.31
wR_2 [a]	0.1754	0.1061	—
wR_1 [b]	—	—	0.0327
R_1 [c]	0.0717	0.0558	0.0315
S_2 [d]	1.139	1.278	—
S_1 [e]	—	—	1.902
$g, g'(w = 1/[\sigma^2(F_o^2) + (gP')^2]$ where $P' = (F_o^2 + 2F_c^2)/3$	0.1165/0.0000	0.0322/2.2354	unit weights

[a] $wR_2 = [\Sigma w(F_o^2 - F_c^2)^2/\Sigma w(F_o^2)^2]^{1/2}$; [b] $wR_1 n = [\Sigma w(F_o - F_c)^2/\Sigma w(F_o)^2]^{1/2}$; [c] $R_1 = \Sigma|F_o - F_c|/\Sigma F_o$; [d] $S_2 = [\Sigma w(F_o^2 - F_c^2)^2/(N - P)]^{1/2}$; [e] $S_1 = [\Sigma w(F_o - F_c)^2/(N - P)]^{1/2}$.

dered into two nearly orthogonal positions. The orientations of all phenyls are defined by the torsion angles quoted in Table 5. The non-bonded energy profiles, obtained by rotating these phenyls about the P–C bonds, show that rotation of phenyl C11 is hindered by its *ortho*- and *meta*-hydrogen atoms and those of phenyl C21, which is hindered by the B conformer of the disordered phenyl C27. Both conformers of this phenyl are hindered in their rotations by the C1A–O1A carbonyl. For the two phenyls attached to P3, rotation of phenyl C31 is hindered by the phenyls C11 and C37, while phenyl C37 is hindered by steric interactions involving phenyl C413 and carbonyl C4A–O4A. The three phenyls attached to P4 are hindered in their rotations by interactions involving the *ortho*-hydrogen atoms: phenyl C41 by phenyl C413 and hydrido H23, phenyl C47 by phenyls C31 and C41, phenyl C413 by phenyl C47.

3. Discussion

3.1. Reactivity of the system investigated

The mononuclear compound (**1**) when heated at 100 °C under hydrogen gives rise to (**2**) by replacement

$Ru_2(CO)_4(MeCO_2)_2(PPh_3)_2$ (4)

↓ T 80°C

$Ru_4(\mu\text{-}H)_4(CO)_9(PPh_3)_3$ (10)

↓ T ⩾ 100°C

$Ru_3(\mu\text{-}H)_2(CO)_8(\mu^3\text{-}PPh)(PPh_3)$ (5)

+

$Ru_3(\mu\text{-}H)(H)(CO)_7(\mu\text{-}PPh_2)_2(PPh_3)$ (6)

+

$Ru_4(CO)_8(\mu^4\text{-}PPh)_2(\mu\text{-}PPh_2)_2$ (7)

+

$Ru_4(\mu\text{-}H)_4(CO)_7(\mu^4\text{-}PPh)(\mu\text{-}PPh_2)_2(PPh_3)$ (8)

Scheme 2.

of the acetato groups with hydridic hydrogens and formation of acetic acid. An intermediate complex containing both a hydrido and an acetato group (**3**) has been identified among the products of the reaction between (**2**) and acetic acid. Under these conditions the mononuclear complex is not transformed into complexes having a higher nuclearity.

The binuclear complex (**4**) reacts with hydrogen giving cluster ruthenium complexes (Scheme 2).

Triphenylphosphine and carbon monoxide ligands are also involved in these transformations. The complexes formed have a higher nuclearity than the starting compound (**4**). With the exception of (**7**) all other complexes contain one or more hydridic hydrogens.

Hydride (**8**) is the main product, at 100 °C, of this reaction. It is a tetranuclear cluster containing four bridging hydridic hydrogen ligands, one monoaryl- and two diarylphosphido ligands. Also, an untouched triphenylphosphine is present. The dearylation of the phosphine ligand is a well-known process [15]. It appears to involve the hydrogenolysis of the P–C bond without hydrogenation of the aromatic ring. In fact, only benzene is recovered from the dearylation of the phosphine.

The first step of these transformations seems to be the loss of acetic acid and the formation of (**10**) as the main product at low temperature (80 °C). This cluster contains only three phosphinic ligands per molecule, indicating that mobilization of the phosphinic ligand and carbon monoxide takes place at the same time. However, working at 100 °C the main product is (**8**) in which one phosphorus atom is linked to each ruthenium atom of the cluster, indicating that different pathways are involved in the synthesis of these complexes.

The formation of (**8**) from (**4**) and hydrogen at 80 °C, even if in a low amount, indicates that the transformation of the phosphinic ligand has already started at a very low temperature in the presence of hydrogen. This behaviour is different from that of the analogous complex with tributylphosphine $Ru_2(CO)_4(MeCO_2)_2(PBu_3)_2$. In fact, using this latter compound the modification of the phosphinic ligand takes place, in the presence of hydrogen, only at 140 °C.

The formation of the phosphido-substituted tri- and tetranuclear clusters, as suggested by Colbran et al. [16], may be associated with the formation of the phosphido ligand having a higher coordination activity than the phosphine.

In Scheme 3 we report two possible paths for aryl elimination from a phosphine bound to a ruthenium atom with formation of the above complexes. Path (a) involves the formation of a ruthenium aryl intermediate by the interaction of a phosphorus–carbon bond of the phosphine with the metal, which is then hydrogenated with elimination of benzene and formation of the hydride. Path (b) involves the hydrogenolysis of a P–C bond followed by benzene elimination and oxidative addition of the P–H bond to the metal atom. Both reaction paths have been suggested previously [4,15,17].

Compound (**4**) behaves differently from the analogous tributylphosphine derivative. In our case we never observe, among the complexes identified, clusters having a nuclearity higher than four, while tributylphosphine complexes give clusters having even six or seven ruthenium atoms. This difference may be connected with the absence of a bare P as ligand in the complexes now synthesized. In fact, as previously suggested [4], the clusters having six or more ruthenium atoms may be a consequence of the formation of an encapsulated phosphorus coordinated to six ruthenium atoms. Using triphenylphosphine, none of the complexes characterized contains an encapsulated phosphorus atom, probably due to the higher stability to hydrogenolysis of the monoarylphosphine compared with the monoalkylphosphine.

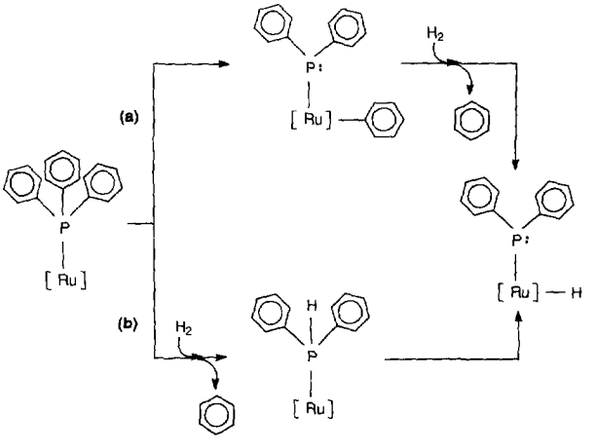

Scheme 3.

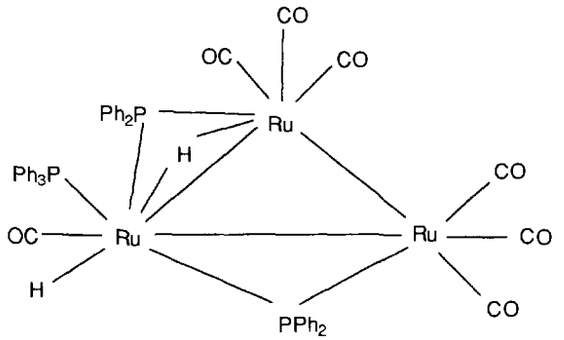

Fig. 4. A picture of the structure attributed to $Ru_3(\mu\text{-}H)(H)(CO)_7(\mu\text{-}PPh_2)_2(PPh_3)$ (**6**).

3.2. NMR spectral properties

3.2.1. $Ru_3(\mu\text{-}H)_2(CO)_8(\mu^3\text{-}PPh)(PPh_3)$ (5)

In the ^{31}P NMR spectrum of compound (**5**) the higher field resonance at 31.9 ppm may be attributed to the phosphine ligand, while the lower one, at 288.9 ppm, may be attributed to the phosphido ligand [18]. The magnetically equivalent hydrides resonate at −18.55 ppm. The chemical shift at high field is in agreement with their bridging position between two ruthenium atoms [19]. The pattern is a doublet of doublets: in fact these hydrides couple with two different phosphorus atoms (one of the phosphine, the other of the phosphido ligand).

3.2.2. $Ru_3(\mu\text{-}H)(H)(CO)_7(\mu\text{-}PPh_2)_2(PPh_3)$ (6)

The resonance at 47.6 ppm in the ^{31}P NMR spectrum of compound (**6**) may be attributed to a triarylphosphine ligand, while the resonance at 93.0 ppm may be attributed to two magnetically equivalent phosphido groups [18]. The two hydrides resonate at −14.47 and −8.89 ppm. The chemical shift at high field suggests that one of the hydrogen atoms is in a bridging position between two ruthenium atoms. The pattern is a doublet of doublets and it couples with two different phosphorus atoms (one of the phosphine, the other of the phosphido ligand). The terminal hydride, that resonates at lower field [19], must be linked to the same ruthenium atom where the triphenylphosphine is linked. In fact, the pattern is a doublet of triplets, because this hydride couples with two magnetically equivalent phosphido groups and one triarylphosphino ligand.

These data suggest, assuming a fluxional behaviour of the hydrides (as suggested by the same chemical shift of the phosphido groups), that a possible structure of compound (**6**) is that reported in Fig. 4.

3.2.3. $Ru_4(CO)_8(\mu^4\text{-}PPh)_2(\mu\text{-}PPh_2)_2$ (7)

In the ^1H NMR spectrum of compound (**7**) no hydride resonance is present. The two resonances in the ^{31}P NMR spectrum may be attributed to the phosphido ligands: presumably, the signal at 189.2 ppm is the PPh_2 ligand and that at 236.6 ppm is the PPh ligand, because a low field resonance is usually due to the less aryl-substituted phosphido ligands [18].

3.2.4. $Ru_4(\mu\text{-}H)_4(CO)_7(\mu^4\text{-}PPh)(\mu\text{-}PPh_2)_2(PPh_3)$ (8)

The ^1H NMR spectrum of compound (**8**) (Table 7) shows four hydridic signals which may be due to four hydrogens coupled with four phosphorus atoms. This hypothesis is confirmed by a GARP experiment (^1H NMR experiment acquired using a broad band ^{31}P decoupling). The patterns of the four resonances are transformed in four singlets.

Each hydride resonance shows a fine structure of a quartet, indicating that each hydride hydrogen is coupled with the other three hydride hydrogens with coupling constants in the range of 1.6–2.0 Hz. This fine structure remains in the GARP experiment.

The ^{31}P NMR spectrum has been attributed on the basis of the following considerations:

— the chemical shift at high field, 51.45 ppm, may be attributed to the PPh_3 group;

— the angle P4–Ru–P1 is 162° as determined by X-ray diffraction (see Fig. 3 for the atom numbering). It is the only angle PRuP very different from 90°, and, as a consequence, the large coupling constant present in

Table 7
NMR data of the complexes [a]

Compound	^{31}P	^1H (hydride region)
(**2**) [b]	57.6 (s, 2P, PPh_3)	−6.35 (t, 2H, J_{HP} 23.4)
(**3**) [b]	46.5 (s, 2P, PPh_3)	−3.68 (t, 1H, J_{HP} 19.2)
(**5**)	31.9 (d, 1P, PPh_3, J_{PP} 118.0), 288.9 (d, 1P, PPh, J_{PP} 118.0)	−18.55 (dd, J_{HP} 10.3, J_{HP} 15.8)
(**6**)	47.6 (t, 1P, PPh_3, J_{PP} 33.6), 93.0 (d, 2P, PPh_2, J_{PP} 33.6)	−14.47 (dd, 1H, J_{HP} 13.6, J_{HP} 12.5), −8.89 (dt, 1H, J_{HP} 9.6, J_{HP} 18.0)
(**7**)	189.2 (t, 2P, PPh_2, J_{PP} 22.1), 236.6 (t, 2P, PPh, J_{PP} 22.1)	
(**8**)	51.5 (dd, 1P, J_{PP} 17.1, PPh_3, J_{PP} 93.2), 68.2 (ddd, 1P, PPh, J_{PP} 24.2, J_{PP} 35.0, J_{PP} 93.2,), 87.6 (t, 1P, PPh_2, J_{PP} 35.0, J_{PP} 35.0), 97.0 (ddd, 1P, PPh_2, J_{PP} 17.1, J_{PP} 24.2, J_{PP} 35.0)	−14.53 (dd, 1H, HRu, J_{HP} 16.5, J_{HP} 26.4), −13.94 (ddd, 1H, HRu, J_{HP} 6.8, J_{HP} 12.3, J_{HP} 27.5), −9.46 (dq, 1H, HRu, J_{HP} 10.5, J_{HP} 19.1), −9.03 (dt, 1H, HRu, J_{HP} 9.3, J_{HP} 16.0)

[a] CD_2Cl_2 solution, chemichal shift in ppm, coupling constants in hertz; s: singlet, d: doublet, t: triplet, q: quartet. [b] C_6D_6 solution.

the spectrum (93.2 Hz) may be attributed to the coupling between P4 and P1;

— the resonance at 68.22 ppm may be attributed to P1.

— in consideration of the previous attributions, the resonance at 96.9 ppm may be attributed to the P3 atom because there is the coupling with P4 (J 16.8 Hz). The angle P3Ru3P4 is 108°;

— finally the last resonance at 87.58 ppm may be attributed to P2.

The coupling constant are: J_{P1P2} 35.0 Hz, J_{P1P3} 24.2 Hz, J_{P1P4} 93.2 Hz, J_{P2P3} 35.0 Hz, J_{P2P4} 0.0 Hz, J_{P3P4} 17.1 Hz.

Carrying out a selective ^{31}P decoupling we can attribute the ^{1}H NMR spectrum as follows:

— the resonance at −9.03 ppm to the H14 because it is a doublet (J 9.3 Hz) of triplets (J 16.0 Hz). In consideration of the structure reported in Fig. 3 this hydrogen may couple with P1, P2, and P3. By ^{31}P selective decoupling we can assign the couplings as J_{HP1} 9.3 Hz, J_{HP2} 16.0 Hz and J_{HP3} 16.0 Hz;

— the resonance at −9.45 ppm to the H23 because it is a doublet (J 10.5 Hz) of quartets (J 19.1 Hz). This hydrogen may couple with P1, P2, P3, and P4. By ^{31}P selective decoupling we can assign the couplings as J_{HP1} 10.5 Hz, J_{HP2} 19.1 Hz, J_{HP3} 19.1 Hz, and J_{HP4} 19.1 Hz;

— the resonance at −13.94 ppm to the H34 because it is a doublet (J 6.8 Hz) of doublet (J 12.3 Hz) of doublets (J 27.5 Hz). In consideration of the structure reported, this hydrogen may couple with P1, P3, and P4. By ^{31}P selective decoupling we can assign the couplings as J_{HP1} 12.3 Hz, J_{HP3} 27.5 Hz, and J_{HP4} 6.8 Hz.

— the resonance at −14.53 ppm to the H12 because it is a doublet (J 16.5 Hz) of doublets (J 26.4 Hz). This hydrogen may couple with P1, and P2. By ^{31}P selective decoupling we can assign the couplings as J_{HP1} 16.5 Hz, J_{HP2} 26.4 Hz.

Wide differences in the ^{31}P chemical shifts of the PPh ligands in the complexes reported have previously been noticed in other cases [20]. Wide differences are also present in the ^{31}P chemical shifts of the PPh_2 ligands.

4. Experimental

Glc analyses were performed with a Perkin–Elmer Model 1022, Autosystem Gas-Chromatograph, using an FFAP column (50 °C for 15 min, then heated to 140 °C at 10 °C min^{-1} and then kept at 140 °C for 15 min).

IR spectra were recorded with a Perkin–Elmer 1760-X FT-IR, using CH_2Cl_2 solutions.

^{1}H, $^{13}C\{^{1}H\}$ and $^{31}P\{^{1}H\}$ NMR spectra were recorded using a Varian VXR300 spectrometer operating at 299.987 MHz for ^{1}H, at 75.429 MHz for ^{13}C NMR and at 121.421 MHz for ^{31}P NMR, using solutions in CD_2Cl_2 or C_6D_6; $SiMe_4$ was used as external standard for ^{1}H NMR and ^{13}C NMR, H_3PO_4 (85%) for ^{31}P NMR (signals reported as positive downfield of the standard). $^{1}H\{^{31}P\}$ NMR experiments were carried out on a Bruker ACP200 (200.13 MHz) instrument equipped with a 5 mm inverse probe and a BFX-5 amplifier device.

X-ray diffraction data were collected as indicated in Table 6.

Compounds $Ru(CO)_2(MeCO_2)_2(PPh_3)_2$ (**1**) [21], $Ru_2(CO)_4(MeCO_2)_2(PPh_3)_2$ (**4**) [22], $Ru_4(\mu\text{-}H)_4(CO)_8(PPh_3)_4$ (**9**) [10], $Ru_4(\mu\text{-}H)_4(CO)_9(PPh_3)_3$ (**10**) [10] and $Ru_3(CO)_9(PPh_3)_3$ (**11**) [23] were synthesized as reported in the literature.

4.1. Synthesis of $Ru(H)_2(CO)_2(PPh_3)_2$ (2)

This compound was synthesized using a modification of the procedure reported by Salvini et al. for the analogous tributylphosphine derivative [6].

In a glass vial sodium carbonate (300 mg) was added to a C_6D_6 (2 ml) solution of complex (**1**) (50 mg, 62.5 mmol). The vial was introduced in a stainless steel autoclave (125 ml) in which a nitrogen atmosphere was created. Hydrogen (100 atm) was introduced in the vessel, then it was heated at 100 °C for 24 h. The autoclave was cooled at room temperature, the reaction product was filtered to eliminate some solid and the solution, containing pure $Ru(H)_2(CO)_2(PPh_3)_2$, was placed in an NMR tube. ^{1}H, ^{31}P and ^{13}C NMR spectra were then recorded. The data obtained indicate a quantitative transformation of (**1**) into (**2**). The solution was then distilled under vacuum to eliminate the solvent, the residue was dissolved in CH_2Cl_2 and analysed by IR spectroscopy. The data of (**2**) are reported in Tables 7 and 8.

4.2. Synthesis of $RuH(CO)_2(MeCO_2)(PPh_3)_2$ (3)

Acetic acid (18 μl, 314.4 μmol) was added to an equimolecular amount of a C_6D_6 (2 ml) solution of (**2**), prepared from (**1**) (26.5 mg, 33.1 μmol). After 21 h the

Table 8
IR data of the complexes in the carbonyl stretching region [a]

Compound	ν (cm^{-1})
(**2**)	2018(s), 1979(s)
(**3**) [b]	2045(s), 1970(s)
(**5**)	2076(w), 2038(s), 2002(m), 1990(m)
(**6**)	2055(w), 2034(s), 1989(s)
(**7**)	2036(w), 2011(s), 1994(m), 1969(m)
(**8**)	2039(w), 2022(s), 1975(s), 1943(sh)

[a] CH_2Cl_2 solution; s: strong, m: medium, w: weak, sh: shoulder. [b] C_6D_6 solution.

conversion of (**2**) into the new product (**3**) was 88.7%, 7.8% of (**1**) was also formed. ^{1}H, ^{31}P and ^{13}C NMR spectra were then recorded. The solvent was distilled under vacuum, the residue dissolved in CH_2Cl_2 and analysed by IR spectroscopy. The data of (**3**) are reported in Tables 7 and 8.

4.3. Reaction of $Ru(H)_2(CO)_2(PPh_3)_2$ with acetic acid

Acetic acid (18 μl, 314.4 μmol) was added at 20 °C to a C_6D_6 (1 ml) solution of (**2**), prepared from (**1**) (26.5 mg, 33.1 μmol). The conversion of (**2**) into (**3**) was followed at 20 °C by recording ^{31}P NMR spectra at various time intervals. The data collected in 90 min indicated a first order reaction with respect to the concentration of (**3**) with a specific rate of 1.8×10^{-4} mol s^{-1}.

4.4. Reaction of $RuH(CO)_2(MeCO_2)(PPh_3)_2$ with acetic acid

Acetic acid (18 μl, 314.4 μmol) was added at 50 °C to a C_6D_6 (1 ml) solution of (**2**), prepared from (**1**) (26.5 mg, 33.1 μmol). The conversion of (**2**) into (**3**) reached 96% in 15 min. The transformation of (**3**) into (**1**) was followed at 50 °C by recording ^{31}P NMR spectra at various time intervals. The data collected in 20 h indicated a first order reaction with respect to the concentration of (**3**) with a specific rate of 3×10^{-5} mol s^{-1}.

4.5. Behaviour of phosphine-substituted ruthenium carbonyls with hydrogen

4.5.1. General procedure

In a stainless steel rocking autoclave (125 ml) equipped with a manometer and a valve, air was replaced by nitrogen, then a solution of the compound in the appropriate solvent was introduced. Hydrogen was added to the desired pressure and the reactor was heated at the prefixed temperature for the time required. The concentration of the solution, the solvent, the hydrogen pressure, the temperature and the reaction time are reported in Tables 1 and 2.

At the end of the reaction the autoclave was cooled, the gas vented and a brown-violet solution was collected and separated from the solid by filtration. The solvent was eliminated by distillation under reduced pressure, an IR spectrum was recorded on a sample dissolved in CH_2Cl_2 and a ^{31}P NMR on another sample in a CD_2Cl_2 solution.

The products were separated by tlc using SiO_2 preparative plates (Merck, 2 mm) having a fluorescent indicator at 254 nm. A solution of 40°–70° petroleum ether–CH_2Cl_2 80/20 was employed as eluent. The elution was repeated three times.

Further purifications of the products were done using the same procedure.

The compounds were crystallized by a CH_2Cl_2–pentane solution by cooling at −20 °C. When appropriate crystals were obtained they were analysed by single crystal X-ray determinations.

The elemental data of the purified products were as follows.

Compound (**5**). Found: C, 42.5; H, 2.4. $C_{32}H_{22}O_8P_2Ru_3$ (Mw = 899.68). Calc.: C, 42.7; H, 2.5%.

Compound (**6**). Found: C, 52.1; H, 3.5. $C_{49}H_{37}O_7P_3Ru_3$ (Mw = 1133.96). Calc.: C, 51.9; H, 3.3%. MS spectrum in the range 1200–900 *m/e* shows peaks at *m/e* 1134 $(M)^+$, 1106 $(M - CO)^+$[100], 1078 $(M - 2CO)^+$, 1050 $(M - 3CO)^+$, 1022 $(M - 4CO)^+$, 994 $(M - 5CO)^+$, 966 $(M - 6CO)^+$, 938 $(M - 7CO)^+$.

Compound (**7**). Found: C, 43.7, H, 2.7. $C_{44}H_{30}O_8P_4Ru_4$ (Mw = 1214.89). Calc.: C, 43.5; H, 2.5.

Compound (**8**). Found: C, 49.0; H, 3.1. $C_{55}H_{44}O_7P_4Ru_4$ (Mw = 1345.13). Calc.: C, 49.1; H, 3.3%.

4.6. Spectroscopic determination of hydridic hydrogens

Owing to the high value of the ratio between aromatic and hydridic hydrogens in compounds (**5**), (**6**) and (**8**), the number of hydridic hydrogens has been evaluated using a $CDCl_3$ solution containing an exact amount of the complex examined and of the reference compound (**9**), having the resonance of hydridic hydrogens different from those of (**5**), (**6**) and (**8**).

A $CDCl_3$ solution of (**5**) 10.3 mg (0.0115 mmol) and (**9**) 12.7 mg (0.0076 mmol) gave the integration of the resonances at −18.55 (dd, 2H) for (**5**) with respect to that at −15.65 (m, 4H) for (**9**), confirming the X-ray attribution.

As reported for (**5**), a $CDCl_3$ solution of (**6**) 19.2 mg (0.0169 mmol) and (**9**) 19.5 mg (0.0116 mmol) gave the integration of the resonances at −14.47 (dd, 1H), −8.89 (dt, 1H) for (**6**) with respect to that at −15.65 (m, 4H) for (**9**).

In the same way, a $CDCl_3$ solution of (**8**) 51.2 mg (0.0382 mmol) and (**9**) 50.0 mg (0.0298 mmol) gave the integration of the resonances at −14.53 (dd, 1H), −13.94 (ddd, 1H), −9.46 (dq, 1H), −9.03 (dt, 1H) for (**8**) with respect to that at −15.65 (m, 4H) for (**9**), confirming the X-ray determination.

4.7. X-ray crystallography

The relevant data for the crystal structure analyses are summarized in Table 6. The lattice parameters were determined with the Mo Kα radiation (λ = 0.71073 Å) and refined by a least squares procedure [24], using the

Nelson and Riley [25] extrapolation function. The integrated intensities were measured at room temperature (293(2) K) with Mo-Kα radiation, using the θ–2θ scan mode and a modified version [26] of the Lehmann and Larsen [27] peak-profile analysis procedure. All reflections were corrected for Lorentz and polarization effects, while correction for absorption was applied by the Ψ-scan method [28] to compound (**7**) (ratio of transmission factors: $T_{max}/T_{min} = 1/0.807 = 1.24$, calculated from the maximum and minimum sizes of the crystal-sample 1.42) and by $\Delta(F)$ refinement [29] for compound (**8**) ($T_{max}/T_{min} = 1/0.794 = 1.26$, calc. 1.69); no absorption correction was applied to the data of compound (**5**).

Table 9
Final atomic coordinates ($\times 10^4$) of non-hydrogen atoms of compound (**5**), with e.s.d.s in parentheses

Atom	x	y	z
Ru1	820.2(5)	−1600.6(6)	−282.7(9)
Ru2	1661.2(5)	−619.8(6)	−1587.7(9)
Ru3	2431.7(5)	−1808.3(6)	55.3(10)
P1	3078(2)	−1288(2)	1970(3)
P2	1558(2)	−1916(2)	−1726(3)
O1	354(7)	−3011(7)	1027(12)
O2	−582(5)	−1480(6)	−2163(10)
O3	380(5)	−331(6)	1417(10)
O4	390(6)	−308(7)	−3673(9)
O5	2881(7)	−150(9)	−3060(13)
O6	1392(6)	801(5)	−55(11)
O7	3751(6)	−2005(8)	−1233(12)
O8	2314(7)	−3415(6)	952(13)
C1C	525(8)	−2490(9)	542(14)
C2C	−61(8)	−1529(8)	−1481(13)
C3C	576(7)	−807(8)	826(12)
C4C	864(8)	−419(8)	−2896(13)
C5C	2416(8)	−318(9)	−2534(14)
C6C	1501(7)	284(8)	−613(12)
C7C	3260(7)	−1947(8)	−685(13)
C8C	2392(8)	−2810(9)	594(15)
C1	1479(7)	−2546(8)	−3062(10)
C2	1963(10)	−2512(9)	−3918(15)
C3	1929(13)	−2988(11)	−4959(18)
C4	1375(12)	−3493(12)	−5180(16)
C5	870(11)	−3566(12)	−4338(18)
C6	900(9)	−3075(10)	−3274(17)
C7	2483(7)	−764(7)	2871(11)
C8	1948(7)	−1175(9)	3418(12)
C9	1463(8)	−764(11)	4044(12)
C10	1505(9)	−15(12)	4118(14)
C11	1998(10)	387(10)	3618(16)
C12	2499(8)	24(8)	2985(15)
C13	3814(8)	−603(7)	1821(14)
C14	4477(7)	−597(9)	2639(18)
C15	5017(9)	−87(12)	2466(24)
C16	4900(11)	447(11)	1544(23)
C17	4257(11)	464(10)	731(20)
C18	3726(9)	−89(9)	864(16)
C19	3554(6)	−1981(8)	3087(13)
C20	3573(8)	−1926(9)	4391(13)
C21	3978(10)	−2427(12)	5229(16)
C22	4320(11)	−3036(12)	4724(22)
C23	4289(10)	−3128(9)	3449(19)
C24	3893(7)	−2594(8)	2614(14)

Table 10
Final atomic coordinates ($\times 10^4$) of non-hydrogen atoms of compound (**7**) with e.s.d.s in parentheses

Atom	x	y	z
Ru1	5002.8(7)	329.3(7)	2089.0(8)
Ru2	3098.0(7)	−1028.9(7)	−815.4(8)
P1	2785(2)	−131(2)	1533(3)
P2	4733(2)	1176(2)	249(3)
O1	5399(8)	−1218(8)	3803(9)
O2	6366(9)	2975(8)	5045(9)
O3	1043(8)	−905(9)	−3176(9)
O4	1663(9)	−3955(7)	−2129(11)
C1C	5258(10)	−633(10)	3148(11)
C2C	5849(11)	1983(9)	3944(12)
C3C	1809(10)	−947(9)	−2264(11)
C4C	2178(10)	−2845(10)	−1610(13)
C1	1836(9)	−1227(9)	2069(11)
C2	927(8)	−899(8)	2783(10)
C3	217(10)	−1761(11)	3141(13)
C4	385(12)	−2963(12)	2796(15)
C5	1270(13)	−3354(12)	2112(16)
C6	2005(11)	−2442(10)	1765(13)
C7	2240(9)	1296(9)	2159(11)
C8	1487(10)	1552(9)	1118(12)
C9	1101(9)	2670(10)	1619(13)
C10	1472(10)	3552(10)	3169(14)
C11	2252(11)	3316(11)	4227(14)
C12	2635(10)	2210(9)	3729(12)
C13	4372(9)	2686(8)	557(11)
C14	3524(10)	2712(10)	−668(13)
C15	3261(11)	3905(12)	−370(16)
C16	3820(13)	4989(11)	1068(19)
C17	4603(14)	4942(11)	2219(16)
C18	4897(10)	3803(9)	2001(13)

The structures were solved by direct methods using SIR92 [30] for compounds (**5**) and (**7**) and SHELXS-86 [31] for compound (**8**). In each case the heaviest atoms and a number of oxygen and carbon atoms were found first, then the other non-hydrogen atoms were localized from successive difference Fourier maps. Refinements for compounds (**5**) and (**7**) were carried out by full-matrix least squares on F^2 using the SHELXL-93 [32] program, while SHELX-76 [33] was used to refine compound (**8**) by block-diagonal least squares on F.

The C27-phenyl ring of compound (**8**) came out to be disorderly distributed into two mutually orthogonal positions (see Fig. 3) with occupancy factors of 0.56 and 0.44 for the C27,C28A,C29A,C210,C11A,C12A and C27,C28B,C29B, C210,C11B,C12B rings respectively. The hydride hydrogens of compounds (**5**) and (**8**) were found in final difference maps, refined isotropically and checked by the HYDEX program [34], while for compound (**7**) no hydride hydrogen was found. The other hydrogen atoms of compound (**5**) and all of compound (**7**) were put in calculated positions, while those of compound (**8**) were found from $\Delta\rho$ maps and

Table 11
Final atomic coordinates ($\times 10^4$) of non-hydrogen atoms of compound (**8**), with e.s.d.s in parentheses

Atom	x	y	z
Ru1	1822.8(2)	131.5(3)	3311.8(4)
Ru2	1510.0(2)	−1226.0(3)	4055.2(4)
Ru3	2726.0(2)	−1281.0(3)	5520.9(3)
Ru4	3031.8(2)	98.0(3)	4835.6(3)
P1	2512.4(7)	−929.0(9)	3778.0(12)
P2	1144.2(7)	−766.0(10)	2463.7(12)
P3	3713.1(7)	−825.9(2)	1718(4)
P4	2615.4(7)	−1497.6(9)	7107.9(12)
O1	2331(3)	842(3)	1718(4)
O1A	840(2)	1303(3)	3200(5)
O2	1415(3)	−2874(3)	3770(5)
O2A	346(3)	−1157(5)	4783(5)
O3	2912(3)	−2905(3)	5300(4)
O4	3720(3)	857(3)	3505(4)
O4A	3418(3)	1313(3)	6338(4)
C1	2135(3)	576(4)	2314(5)
C1A	1218(3)	870(4)	3236(5)
C2	1456(3)	−2255(5)	3867(5)
C2A	780(3)	−1185(5)	4498(5)
C3	2839(3)	−2292(4)	5393(5)
C4	3463(3)	560(4)	4004(5)
C4A	3280(3)	845(4)	5771(5)
C11	2862(3)	−1391(3)	2893(4)
C12	2705(3)	−2123(4)	2613(5)
C13	2970(4)	−2458(4)	1916(6)
C14	3371(4)	−2091(5)	1501(5)
C15	3525(3)	−1374(4)	1783(5)
C16	3270(3)	−1023(4)	2460(4)
C21	1315(3)	−1275(4)	1451(4)
C22	1683(3)	−1004(4)	870(5)
C23	1794(4)	−1401(5)	97(6)
C24	1559(4)	−2088(5)	−117(6)
C25	1208(4)	−2372(4)	459(7)
C26	1076(4)	−1986(4)	1235(5)
C27	318(3)	−557(4)	1965(5)
C28A	−121(7)	−974(9)	2118(11)
C28B	−39(8)	−358(10)	2580(13)
C29A	−750(8)	−815(10)	1683(12)
C29B	−690(10)	−246(12)	2230(16)
C210	−917(4)	−281(7)	1169(9)
C11A	−459(7)	264(8)	959(10)
C11B	−648(13)	−625(15)	644(19)
C12A	163(5)	104(7)	1386(9)
C12B	−14(9)	−760(11)	991(14)
C31	4195(3)	−1252(4)	4925(4)
C32	4210(3)	−2007(4)	4801(7)
C33	4567(4)	−2308(5)	4208(8)
C34	4915(4)	−1876(6)	3778(7)
C35	4901(3)	−1142(6)	3898(6)
C36	4542(3)	−821(4)	4453(5)
C37	4276(3)	−596(3)	6818(4)
C38	4889(3)	−838(4)	7052(5)
C39	5291(3)	−668(5)	7939(6)
C310	5109(4)	−242(6)	8609(5)
C311	4499(4)	1(5)	8415(5)
C312	4089(3)	−172(4)	7527(5)
C41	1831(3)	−1851(4)	7037(4)
C42	1387(3)	−1467(5)	7357(5)
C43	795(4)	−1746(6)	7206(7)
C44	635(4)	−2389(7)	6720(7)
C45	1062(4)	−2787(5)	6407(7)
C46	1658(3)	−2522(4)	6559(6)
C47	2683(3)	−710(3)	7946(4)
C48	3016(3)	−736(4)	8929(5)
C49	3069(4)	−120(4)	9540(5)
C410	2776(4)	529(4)	9172(6)
C411	2453(3)	566(4)	8194(6)
C412	2403(3)	−38(4)	7575(5)
C413	3113(3)	−2197(3)	7875(4)
C414	3731(4)	−2246(5)	7860(6)
C415	4114(4)	−2731(6)	8474(8)
C416	3900(4)	−3199(5)	9074(7)
C417	3294(4)	−3158(4)	9091(5)
C418	2902(3)	−2657(4)	8492(5)

refined, except those of the disordered phenyl which were put in calculated positions.

All calculations were carried out on the ENCORE-91 and POWERNODE-6040 computers of the "Centro di Studio per la Strutturistica Diffrattometrica del C.N.R. (Parma)". In addition to the quoted programs, PARST [35] was used for the calculations concerning the geometrical aspects of the crystal structures.

Atomic scattering factors and anomalous-scattering coefficients were taken from the *International Tables for X-Ray Crystallography* [36]. Final fractional coordinates are quoted in Tables 9–11.

Hydrogen atom coordinates, bond lengths and angles, thermal parameters and torsion angles have been deposited at the Cambridge Crystallographic Data Centre. Structural factors are available from the authors (S.I., M.N.).

The averaged values quoted in Tables 3–5 are means weighted according to the reciprocal of the variances, and the corresponding estimated standard deviations (e.s.d.s) are the largest of the values of the 'external' and 'internal' standard deviations [37].

Acknowledgements

Thanks are due to Dr. Maurizio Peruzzini, ISSEC-Firenze for the aid in the NMR-GARP experiments. The authors are indebted to the Ministero della Ricerca Scientifica e Tecnologica (MURST) for financial support (40% and 60%).

References

[1] (a) P. Frediani, U. Matteoli, M. Bianchi, F. Piacenti and G. Menchi, *J. Organomet. Chem., 150* (1978) 273. (b) U. Matteoli, M. Bianchi, G. Menchi, P. Frediani and F. Piacenti, *J. Mol. Catal., 22* (1984) 353. (c) U. Matteoli, G. Menchi, M. Bianchi, P. Frediani and F. Piacenti, *Gazz. Chim. Ital., 115* (1985) 603. (d) F. Piacenti, P. Frediani, U. Matteoli, G. Menchi and M. Bianchi, *Chim. Ind. (Milan), 68* (1986) 53.

[2] (a) M. Bianchi, G. Menchi, P. Frediani, F. Piacenti, A. Scrivanti and U. Matteoli, *J. Mol. Catal., 50* (1989) 277. (b) P. Frediani, M. Bianchi, F. Piacenti, S. Ianelli and M. Nardelli, *Inorg. Chem., 26* (1987) 1592. (c) C. Bianchini, C. Bohanna, M.A. Esteruelas, P. Frediani, A. Meli, L.A. Oro and M. Peruzzini, *Organometallics, 11* (1992) 3837. (d) P. Frediani, A. Salvini, M. Bianchi and F. Piacenti, *J. Organomet. Chem., 454* (1993) C17. (e) A. Salvini, P. Frediani, D. Rovai, M. Bianchi and F. Piacenti, *J. Mol. Catal., 89* (1994) 77.

[3] P. Frediani, M. Bianchi, A. Salvini, F. Piacenti, S. Ianelli and M. Nardelli, *J. Chem. Soc. Dalton Trans.*, (1990) 165.

[4] P. Frediani, M. Bianchi, A. Salvini, F. Piacenti, S. Ianelli and M. Nardelli, *J. Chem. Soc. Dalton Trans.*, (1990) 1705.

[5] P. Frediani, M. Bianchi, A. Salvini and F. Piacenti, *J. Chem. Soc. Dalton Trans.*, (1990) 3663.

[6] A. Salvini, P. Frediani, M. Bianchi and F. Piacenti, *Inorg. Chim. Acta, 227* (1994) 247.

[7] S. Cenini, F. Porta and M. Pizzotti, *Inorg. Chim. Acta, 20* (1976) 119.

[8] C.L. Lee, J. Chisholm, B.R. James, D.A. Nelson and M.A. Lilga, *Inorg. Chim. Acta, 121* (1986) L7.

[9] F. L'Eplattenier and F. Calderazzo, *Inorg. Chem., 7* (1968) 2162.

[10] F. Piacenti, M. Bianchi, P. Frediani and E. Benedetti, *Inorg. Chem., 10* (1971) 2759.

[11] C.K. Johnson, ORTEP, *Rep. ORNL-3794*, 1965 (Oak Ridge National Laboratory, Tennessee). L. Zsolnai and H. Pritzkow, ZORTEP. ORTEP original program modified for PC, University of Heidelberg, Germany, 1994.

[12] A.G. Orpen, L. Brammer, F.H. Allen, O. Kennard, D.G. Watson and R. Taylor, *J. Chem. Soc. Dalton Trans.*, (1989) S1.

[13] F.H. Allen, O. Kennard, D.G. Watson, L. Brammer, A.G. Orpen and R. Taylor, *J. Chem. Soc. Perkin Trans. II*, (1987) S1.

[14] M. Nardelli, *QCPE Bulletin, QCMP097* (1991) 11; xvii.

[15] A.H. Koelle, in R.B. King (ed.), *Encyclopedia of Inorganic Chemistry*, Vol. 7, Wiley, Chichester, 1994, p. 3549. (b) A.J. Deming, in E.W. Abel, F.G.A. Stone and G. Wilkinson (eds.), *Comprehensive Organometallic Chemistry II*, Vol. 7, Pergamon, 1995, p. 737 and references cited therein. (c) M.P. Cifuentes and M.G. Humphrey, in E.W. Abel, F.G.A. Stone and G. Wilkinson (eds.), *Comprehensive Organometallic Chemistry II*, Vol. 7, Pergamon, 1995, p. 938 and references cited therein.

[16] S.B. Colbran, B.F.G. Johnson, J. Lewis and R.M. Sorrell, *J. Chem. Soc. Chem. Commun.*, (1986) 525.

[17] (a) C. Bergounhou, J.-J. Bonnet, P. Fompeyrine, G. Lavigne, N. Lugan and F. Mansilla, *Organometallics, 5* (1986) 60. (b) P.E. Garrou, *Chem. Rev., 85* (1985) 171.

[18] (a) R.K. Pomeroy, in E.W. Abel, F.G.A. Stone and G. Wilkinson (eds.), *Comprehensive Organometallic Chemistry II*, Vol. 7, Pergamon, 1995, p. 856 and references cited therein.

[19] R.H. Crabtree, in R.B. King (ed.), *Encyclopedia of Inorganic Chemistry*, Vol. 3, Wiley, Chichester, 1994, p. 1392.

[20] (a) F.S. Livotto, P.R. Raithby and M.D. Vargas, *J. Chem. Soc. Dalton Trans.*, (1993) 1797. (b) B.F.G. Johnson, T.M. Layer, J. Lewis, P.R. Raithby and W.-T. Wong, *J. Chem. Soc. Dalton Trans.*, (1993) 973.

[21] (a) B.F.G. Johnson, R.D. Johnson, J. Lewis and I.G. Williams, *J. Chem. Soc. A*, (1971) 689. (b) S.D. Robinson and M.F. Uttley, *J. Chem. Soc. Dalton Trans.*, (1973) 1912. (c) A. Dobson, S.D. Robinson and M.F. Uttley, *J. Chem. Soc. Dalton Trans.*, (1975) 370.

[22] G.R. Crooks, B.F.G. Johnson, J. Lewis, I.G. Williams and G. Gamlen, *J. Chem. Soc. A*, (1969) 2761.

[23] F. Piacenti, M. Bianchi, E. Benedetti and G. Braca, *Inorg. Chem., 7* (1968) 1815.

[24] M. Nardelli and A. Mangia, *Ann. Chim. (Rome), 74* (1984) 163.

[25] J.B. Nelson and D.P. Riley, *Proc. Phys. Soc. London, 57* (1945) 160; 477.

[26] D. Belletti, F. Ugozzoli, A. Cantoni and G. Pasquinelli, *Internal Rep. 1-3/79*, 1979 (Centro di Studio per la Strutturistica Diffrattometrica del CNR, Parma, Italy).

[27] M.S. Lehmann and F.K. Larsen, *Acta Crystallogr. Sect. A:, 30* (1974) 580.

[28] A.C.T. North, D.C. Phillips and F.S. Mathews, *Acta Crystallogr. Sect. A:, 24* (1968) 351.

[29] N. Walker and D. Stuart, *Acta Crystallogr. Sect. A:, 39* (1983) 158.

[30] A. Altomare, G. Cascarano, C. Giacovazzo, A. Guagliardi, M.C. Burla, G. Polidori and M. Camalli, *J. Appl. Cryst., 27* (1994) 435.

[31] G.M. Sheldrick, SHELXS-86, *Program for Crystal Structure Solution*, University of Göttingen, Germany, 1986.

[32] G.M. Sheldrick, SHELXL-93, *Program for Crystal Structure Refinement*, University of Göttingen, Germany, 1992.

[33] G.M. Sheldrick, SHELX-76, *Program for Crystal Structure Determination*, University of Cambridge, UK, 1976.

[34] A.G. Orpen, *J. Chem. Soc. Dalton Trans.*, (1980) 2509.

[35] M. Nardelli, *Comput. Chem., 7* (1983) 95; *J. Appl. Crystallogr., 28* (1995) 659.

[36] International Union of Crystallography, *International Tables for Crystallography*, Vol. C, Kluwer, Dordrecht, 1992, Tables 4.2.6.8, 6.1.1.4.

[37] H. Topping, *Errors of Observation and Their Treatment*, Chapman and Hall, London, 1960, p. 87; 91.